

Modeling Morphology of Social Network Cascades

M. Zubair Shafiq and Alex X. Liu

Department of Computer Science and Engineering, Michigan State University, East Lansing, MI, USA
{shafiqmu,alexliu}@cse.msu.edu

ABSTRACT

Cascades represent an important phenomenon across various disciplines such as sociology, economy, psychology, political science, marketing, and epidemiology. An important property of cascades is their morphology, which encompasses the structure, shape, and size. However, cascade morphology has not been rigorously characterized and modeled in prior literature. In this paper, we propose a Multi-order Markov Model for the Morphology of Cascades (M^4C) that can represent and quantitatively characterize the morphology of cascades with arbitrary structures, shapes, and sizes. M^4C can be used in a variety of applications to classify different types of cascades. To demonstrate this, we apply it to an unexplored but important problem in online social networks – cascade size prediction. Our evaluations using real-world Twitter data show that M^4C based cascade size prediction scheme outperforms the baseline scheme based on cascade graph features such as edge growth rate, degree distribution, clustering, and diameter. M^4C based cascade size prediction scheme consistently achieves more than 90% classification accuracy under different experimental scenarios.

Categories and Subject Descriptors

C.4 [Computer System Organization]: Performance of Systems—*Modeling techniques*; J.4 [Computer Applications]: Social and Behavioral Sciences

General Terms

Experimentation, Measurement, Theory

Keywords

Cascades, Markov Chains, Social Networks

1. INTRODUCTION

1.1 Background and Motivation

The term *cascade* describes the phenomenon of something propagating along the links in a social network. That something can be information such as a URL, action such as a monetary donation, influence such as buying a product, discussion such as commenting on a blog article, and a resource such as a torrent file. Based on what is being propagated, we can categorize cascades into various classes such as information cascades [6], action cascades [8], influence cascades [20], discussion cascades [13], and resource cascades [33]. Consider a toy example where user A , connected to users B and C in a social network, broadcasts a piece of information (*e.g.* a picture or a news article) to his neighbors. Users B and C , after receiving it from user A , may further rebroadcast it to their neighbors resulting in the formation of a cascade.

Cascade phenomenon has been a fundamental topic in many disciplines such as sociology, economy, psychology, political science, marketing, and epidemiology with research literature tracing back to the 1950s [30]. A key challenge in these studies is the lack of large scale cascade data. As online social networks have recently become a primary way for people to share and disseminate information, the massive amount of data available on these networks provides unprecedented opportunities to study cascades at a large scale. Recent events, such as the Iran election protests, Arab Spring, Japanese earthquake, and London riots, have been significantly impacted by campaigns via cascades in online social networks [36, 27, 10]. Studying cascades in online social networks will benefit a variety of domains such as social campaigns [36], product marketing and adoption [25], online discussions [13], sentiment flow [26], URL recommendation [29], and meme tracking [14].

1.2 Problem Statement

The goal of this paper is to study the morphology of cascades in online social networks. Cascade morphology encompasses many aspects of cascades such as their structures, shapes, and sizes. Specifically, we aim to develop a model that allows us to *represent* and *quantitatively characterize* cascade morphology; which are extremely difficult without a model. There are two important requirements on the desired model of cascade morphology. First, this model should have enough expressivity and scalability to allow us to represent and describe cascades with arbitrary structures, shapes, and sizes. Real-world cascades sometimes have large sizes, containing thousands of nodes and edges [22]. Second, this

Permission to make digital or hard copies of all or part of this work for personal or classroom use is granted without fee provided that copies are not made or distributed for profit or commercial advantage and that copies bear this notice and the full citation on the first page. To copy otherwise, to publish, to post on servers or to redistribute to lists, requires prior specific permission and/or a fee.

Copyright 2013 ACM X-XXXXX-XX-X/XX/XX ...\$10.00.

model should allow us to quantitatively characterize and rigorously analyze cascades based on the features extracted from this model.

1.3 Limitations of Prior Art

Despite the numerous publications regarding different aspects of online social networks, little work has been done on the morphology of cascades. Recently some researchers have studied the structure of cascades [23, 22, 36, 13]; however, their analysis of cascade structures is limited to basic structural properties such as degree distribution, size, and depth. These structural properties of cascades are important; however, they are far from being sufficient to precisely describe and represent cascade morphology.

1.4 Proposed Model

In this paper, we propose a Multi-order Markov Model for the Morphology of Cascades (M^4C) that can represent and quantitatively characterize the morphology of cascades with arbitrary structures, shapes, and sizes. M^4C has two key components: a cascade encoding algorithm and a cascade modeling method. The cascade encoding algorithm uniquely encodes the morphology of a cascade for quantitative representation. It encodes a cascade by first performing a depth-first traversal on the cascade graph and then compressing the traversal results using run-length encoding. The cascade modeling method models the run-length encoded sequence of a cascade as a discrete random process. This random process is further modeled as a Markov chain, which is then generalized into a multi-order Markov chain model. M^4C satisfies the aforementioned two requirements. First, this model can precisely represent cascades with arbitrary structures, shapes, and sizes. Second, this model allows us to quantitatively characterize cascades with different attributes using the state information from the underlying multi-order Markov chain model.

1.5 Experimental Evaluation

To demonstrate the effectiveness of our M^4C model in quantitatively characterizing cascades, we use it to investigate an unexplored but important problem in online social networks – *cascade size prediction: given the first τ_1 edges in a cascade, we want to predict whether the cascade will have a total of at least τ_2 ($\tau_2 > \tau_1$) edges over its lifetime*. This prediction has many real-world applications. For example, media companies can use it to predict social media stories that can potentially go viral [15, 29]. Furthermore, solving this problem enables early detection of epidemic outbreaks and political crisis. Despite its importance, this problem has not been addressed in prior literature.

We validate the effectiveness of M^4C based cascade size prediction scheme on a real-world data set collected from Twitter containing more than 8 million tweets, involving more than 200 thousand unique users. The results show that our M^4C based cascade size prediction scheme consistently achieves more than 90% classification accuracy under different experimental scenarios. We also compare our M^4C based cascade size prediction scheme with a baseline prediction scheme based on cascade graph features such as edge growth rate, degree distribution, clustering, and diameter. The results show that M^4C allows us to achieve significantly better classification accuracy than the baseline method.

1.6 Key Contributions

In this paper, we not only propose the first cascade morphology model, but also propose the first cascade size prediction scheme based on our model. In summary, we make the following key contributions in this paper.

1. We propose M^4C for representing and quantitatively characterizing the morphology of cascades with arbitrary structures, shapes, and sizes.
2. To demonstrate the effectiveness of our M^4C model in quantitatively characterizing cascades, we develop a cascade size prediction scheme based on M^4C features and compare its performance with that based on non- M^4C features.

The rest of this paper proceeds as follows. We first review related work in Section 2. We then introduce our proposed model in Section 3. We describe the details of our Twitter data set in Section 4. We present the experimental results of the aforementioned application in Section 5. Finally, we conclude in Section 6 with an outlook to our future work.

2. RELATED WORK

Cascades in online social networks have attracted much attention and investigation; however, little work has been done on cascade morphology. Below we summarize the prior work related to cascade morphology.

2.1 Shape

Zhou *et al.* studied Twitter posts (*i.e.*, tweets) about the Iranian election [36]. In particular, they studied the frequency of pre-defined shapes in cascades. Their experimental results showed that cascades tend to have more width than depth. The largest cascade observed in their data has a depth of seven hops. Leskovec *et al.* studied patterns in the shapes and sizes of cascades in blog and recommendation networks [24, 23]. Their work is also limited to studying the frequency of fixed shapes in cascades.

2.2 Structure

Kwak *et al.* investigated the audience size, tree height, and temporal characteristics of the cascades in a Twitter data set [22]. Their experimental results showed that the audience size of a cascade is independent of the number of neighbors of the source of that cascade. They found that about 96% of the cascades in their data set have a height of 1 hop and the height of the biggest cascade is 11 hops. They also found that about 10% of cascades continue to expand even after one month since their start. Romero *et al.* specifically studied Twitter cascades with respect to hashtags in terms of degree distribution, clustering, and tie strengths [31]. The results of their experiments showed that cascades from diverse topics (identified using hashtags), such as sports, music, technology, and politics, have different characteristics. Similarly, Rodrigues *et al.* studied structure-related properties of Twitter cascades containing URLs [29]. They studied cascade properties like height, width, and the number of users for cascades containing URLs from different web domains. Sadikov *et al.* investigated the estimation of the sizes and depths of information cascades with missing data [32]. Their estimation method uses multiple features including the number of nodes, the number of edges, the number

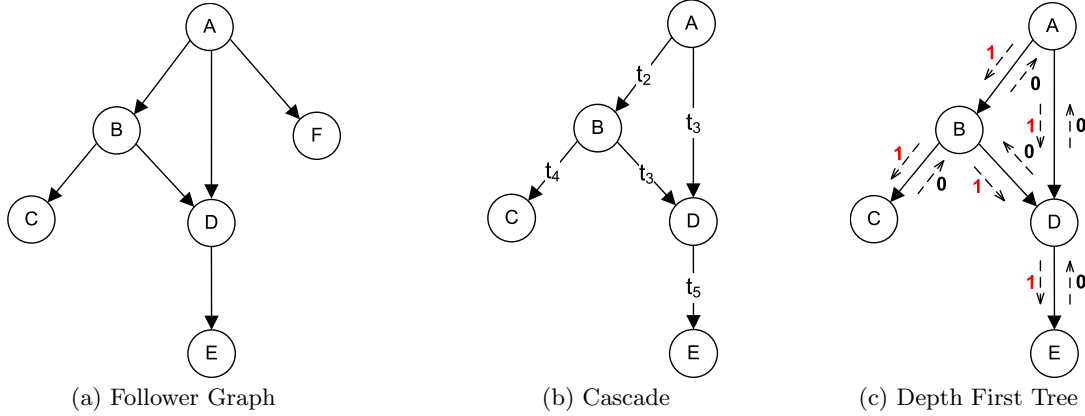


Figure 1: Toy example of cascade construction and encoding.

of isolated nodes, the number of weakly connected components, node degree, and non-leaf node out-degree. Their empirical evaluation using a Twitter data set showed that their method accurately estimates cascade properties for varying fractions of missing data.

2.3 Simulation

Gomez *et al.* studied the structure of discussion cascades in Wikipedia, Slashdot, Barrapunto, and Meneame using features solely based on the depth and degree distribution of cascades [13]. They also developed a generative model based on the maximum likelihood estimation of preferential attachment process to simulate synthetic discussion cascades. However, their model does not capture morphological properties of cascades and is limited to generation of synthetic discussion cascades.

3. PROPOSED MODEL

In this section, we present M^4C for quantitatively representing the morphology of cascades in online social networks. It consists of two major components. The first component encodes a given cascade graph for quantitative representation such that its morphological information is retained. The second component models the encoded sequence using a multi-order Markov chain. Before we describe these two components, we first present the details of the cascade graph construction process.

3.1 Cascade Graph Construction

A social network can be represented using two graphs, a relationship graph and a cascade graph. Both graphs share the same set of nodes (or vertices) V , which represents the set of all users in a social network. A *relationship graph* represents the relationships among users in a social network. In this graph, nodes represent users and edges represent the relationship among users. If the edges are directed, where a directed edge from user u to user v denotes that v is a follower of u , then this graph is called a *follower graph*, denoted as (V, \vec{E}_f) , where V is the set of users and \vec{E}_f is the set of directed edges. If the edges are undirected, where an undirected edge between user u and user v denotes that u and v are friends, then this graph is called a *friendship graph*,

denoted as (V, E_f) , where V is the set of users and E_f is the set of undirected edges. By the nature of our study, we focus on the follower graph denoted as $G_f = (V, \vec{E}_f)$. The *cascade graph* represents the dynamic activities that are taking place in a social network (such as users sharing a URL or joining a group). A cascade graph is an acyclic directed graph denoted as $G_c = (V, \vec{E}_c, T)$ where V is the set of users, \vec{E}_c is a set of directed edges where a directed edge $e = (u, v)$ from user u to user v represents the propagation of something from u to v , and T is a function whose input is an edge $e \in \vec{E}_c$ and output is the time when the propagation along edge e happens.

While the static relationship graph is easy to construct from a social network, the dynamic cascade graph is non-trivial to construct because there maybe multiple propagation paths from the cascade source to a node. So far there is no consensus on cascade graph construction in prior literature. In this paper, we use a construction method that is similar to the method described in [32]. We next explain our construction method through a Twitter example. Consider the follower graph in Figure 1(a). Let (u, t) denote a user u performing an action, such as posting a URL on u 's Twitter profile, at time t . Suppose the following actions happen in the increasing time order: (A, t_1) , (B, t_2) , (D, t_3) , (C, t_4) , (E, t_5) , where $t_1 < t_2 < t_3 < t_4 < t_5$. Suppose (A, t_1) denotes that A posts a URL on his Twitter profile, and all other actions (namely (B, t_2) , (D, t_3) , (C, t_4) , and (E, t_5)) are reposting the same URL from A .

The cascade graph regarding the propagation of this URL is constructed as follows. First, A is the root of the cascade graph because it is the origin of this cascade. Second, B reposting A 's tweet (which is a URL in this example) at time t_2 must be under A 's influence because there is only one path from A to B in the follower graph in Figure 1(a). Therefore, in the cascade graph in Figure 1(b), there is an edge from A to B with time stamp t_2 . Note that each repost (or retweet in Twitter's terminology) contains the origin of the tweet (A in this example). Third, however, D reposting A 's tweet at time t_3 could be under either A 's influence (because there is a path from A to D in the follower graph in Figure 1(a) and $t_1 < t_3$) or B 's influence (because there is a path from B to D in the follower graph as well and $t_2 < t_3$).

Note that even if D sees A 's tweet through B 's retweet, the repost of A 's tweet on D 's profile does not contain any information about B and only shows that the origin of the tweet is A . In this scenario, we assume that D is partially influenced by both A and B , instead of assuming that D is influenced by either user B or A , because this way we can retain more information with respect to the corresponding follower graph. Therefore, there is an edge from A to D and another edge from B to D in the cascade graph shown in Figure 1(b), where the time stamps of both edges are t_3 . Similarly, we add the edge from B to C with a time stamp t_4 and the edge from D to E with a time stamp t_5 in the cascade graph.

3.2 Cascade Encoding

The first step in cascade encoding is to encode the constructed cascade graph as a binary sequence that uniquely represents the structure of the cascade graph. Graph encoding has been studied for a wide range of problems across several domains such as image compression, text and speech recognition, and DNA profiling [28, 3, 16]. The typical goal of graph encoding is to transform large geometric data into a succinct representation for efficient storage and processing. However, our goal here is to encode a given cascade graph in a way that its morphological information is captured. Towards this end, we use the following graph encoding algorithm.

We first conduct a depth-first traversal of the constructed cascade graph starting from the root node, which results in a spanning tree. To result in a unique spanning tree, at each node in the cascade graph, we sort the outgoing edges in the increasing order of their time stamps, *i.e.*, sort the outgoing edges e_1, e_2, \dots, e_k of a node so that $T(e_1) < T(e_2) < \dots < T(e_k)$; and then traverse them in this order. For each edge, we use 1 to encode its downward traversal and 0 to encode its upward traversal. Figure 1(c) shows the traversal of the cascade graph in Figure 1(b) and the encoding of each downward or upward traversal. The binary encoding results from this traversal process is **11011000**. Let C represent the binary code of a cascade graph $G = (V, \vec{E})$. Then the length of the binary code $|C|$ is always twice the size of the edge set $|\vec{E}|$, *i.e.*, $|C| = 2|\vec{E}|$. Furthermore, let $C[i]$ be the i -th element of the binary code and $I(C[i])$ be an indicator function so that $I(C[i]) = 1$ if $C[i] = 1$, and $I(C[i]) = -1$ if $C[i] = 0$. Because each edge is exactly traversed twice, one downward and one upward, we have:

$$\sum_{i=1}^{|C|} I(C[i]) = 0.$$

The second step in cascade encoding is to convert the binary sequence, which is obtained from the depth-first traversal of the cascade graph, into the corresponding run-length encoding. A *run* in a binary sequence is a subsequence where all bits in this subsequence are 0s (or 1s) but the bits before and after the subsequence are 1s (or 0s), if they exist. By replacing each run in a binary sequence with the length of the run, we obtain the run-length encoding of the binary sequence [19]. For example, for the binary sequence **11011000**, the corresponding run-length encoding is **2123**. Since the binary sequence obtained from our depth-first traversal of a cascade graph always starts with 1, the run-length encoding uniquely and compactly represents the binary sequence.

3.3 Markov Chain Model of Cascades

We want to model cascade encoding to capture characteristics of cascades so that they can be used to identify the similarities and differences among cascades. This model should allow us to extract morphological features for different classes of cascades and then use these features to classify them. We first present our model, and then demonstrate its usefulness in classifying cascades.

Consider the run-length encoded sequence \hat{C} of a cascade graph G . We can model this sequence using a discrete random process $\{\hat{C}_k\}$, $k = 1, 2, \dots, |\hat{C}|$. Basic analysis of this process reveals that there is some level of dependencies among the consecutive symbols emitted by the random process. In other words, it would be unreasonable to assume that the process is independent or memoryless. Meanwhile, to balance between capturing some of the dependencies within the process and to simplify the mathematical treatment of this encoded sequence, we resort to invoking the Markovian assumption [5]. As we show later, this assumption can be reasonably justified (to some extent) by analyzing the autocorrelation function of the underlying process $\{\hat{C}_k\}$. For a first order Markov process, this implies the following assumption: $Pr[\hat{C}_n = c_n | \hat{C}_1 = c_1, \hat{C}_2 = c_2, \dots, \hat{C}_{n-1} = c_{n-1}] = Pr[\hat{C}_n = c_n | \hat{C}_{n-1} = c_{n-1}]$. Equivalently:

$$Pr[c_1, c_2, \dots, c_n] = Pr[c_1]Pr[c_2|c_1] \dots Pr[c_n|c_{n-1}]. \quad (1)$$

In other words, we invoke the Markovian assumption about the underlying cascade process and its morphology, which is represented by the encoded sequence \hat{C} .

Given the Markovian assumption with homogeneous time-invariant transition probabilities, \hat{C} can be represented using a traditional Markov chain. Figure 2 shows the Markov chain corresponding to the toy example in Figure 1, where each unique symbol in \hat{C} is represented as a state. The Markov chain in Figure 2 has 3 states because there are 3 unique symbols in its run-length encoding.

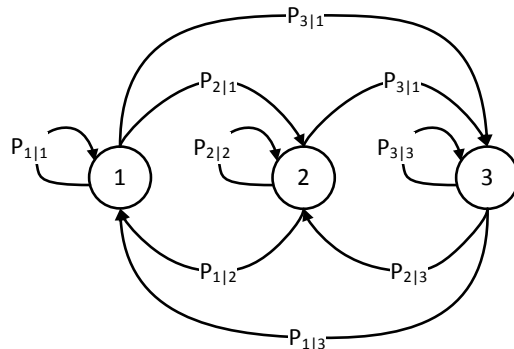


Figure 2: Markov chain model for the toy example.

A Markov chain can also be specified in terms of its state transition probabilities, denoted as T . Hence, for the toy example of Figure 2, we have:

$$T = \begin{pmatrix} P_{1|1} & P_{1|2} & P_{1|3} \\ P_{2|1} & P_{2|2} & P_{2|3} \\ P_{3|1} & P_{3|2} & P_{3|3} \end{pmatrix},$$

where $P_{i|j}$ represents the conditional probabilities $Pr[\hat{C}_n = i | \hat{C}_{n-1} = j]$. The Markov chain framework allows us to quan-

tify the probability of an arbitrary sequence of states by using Equation 1. This will help us to identify sequences that are more (or less) probable in one class of cascades. We next further generalize the above basic Markov chain model.

3.4 Multi-order Generalization

Each element of the state transition matrix of a Markov chain is equivalent to a sub-sequence of \hat{C} , which in turn is equivalent to a subgraph of the corresponding cascade. We can generalize a Markov chain model by incorporating multiple consecutive transitions as a single state in the state transition matrix, which will allow us to specify arbitrary sized subgraphs of cascades. Such generalized Markov chains are called multi-order Markov chains and are sometimes referred to as full-state Markov chains [21]. The order of a Markov chain represents the extent to which past states determine the present state. The basic Markov chain model introduced earlier is of order 1.

Autocorrelation is an important statistic for selecting appropriate order for a Markov chain model [5]. For a given lag t , the autocorrelation function of a stochastic process, X_m (where m is the time or space index), is defined as:

$$\rho[t] = \frac{E\{X_0 X_t\} - E\{X_0\}E\{X_t\}}{\sigma_{X_0} \sigma_{X_t}}, \quad (2)$$

where $E(\cdot)$ represents the expectation operation and σ_{X_i} is the standard deviation of the random variable at time or space lag i . The value of the autocorrelation function lies in the range $[-1, 1]$, where $|\rho[t]| = 1$ indicates perfect correlation at lag t and $\rho[t] = 0$ means no correlation at lag t . Figure 3 plots the sample autocorrelation function of the run-length encoding of an example cascade. The dashed horizontal lines represent the 95% confidence envelope. For this particular example, we observe that sample autocorrelation values jump outside the confidence envelope at lag = 3. This indicates that the underlying random process has the third order dependency. Thus, we select the third order for Markov chain model for this particular cascade. The autocorrelation-based analysis of more complex cascades can lead to even higher order Markov chains.

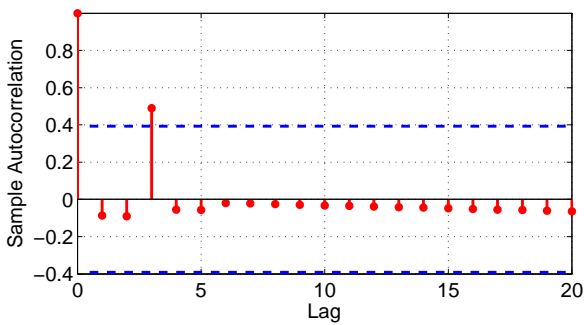


Figure 3: Sample autocorrelation function for the toy example.

The number of possible states of a Markov chain increase exponentially with an increase in the order of the Markov chain model. For the n -th order extension of a Markov chain with k states, the total number of states is k^n . Figure 4 shows

the plot of the second order extension of the 3-state, 1-st order Markov chain model shown in Figure 2. This second order Markov chain contains a total of $3^2 = 9$ states, 4 of which are shown in the figure due to space limitations. In this second order Markov chain model, the conditional probabilities are in the form $P_{i,j|k,l}$ and the state transition matrix is now defined as follows.

$$T_2 = \begin{pmatrix} P_{1,1|1,1} & P_{1,1|1,2} & P_{1,1|1,3} & \dots & P_{1,1|3,3} \\ P_{1,2|1,1} & P_{1,2|1,2} & P_{1,2|1,3} & \dots & P_{1,2|3,3} \\ P_{1,3|1,1} & P_{1,3|1,2} & P_{1,3|1,3} & \dots & P_{1,3|3,3} \\ \vdots & \vdots & \vdots & \ddots & \vdots \\ P_{3,2|1,1} & P_{3,2|1,2} & P_{3,2|1,3} & \dots & P_{3,2|3,3} \\ P_{3,3|1,1} & P_{3,3|1,2} & P_{3,3|1,3} & \dots & P_{3,3|3,3} \end{pmatrix}$$

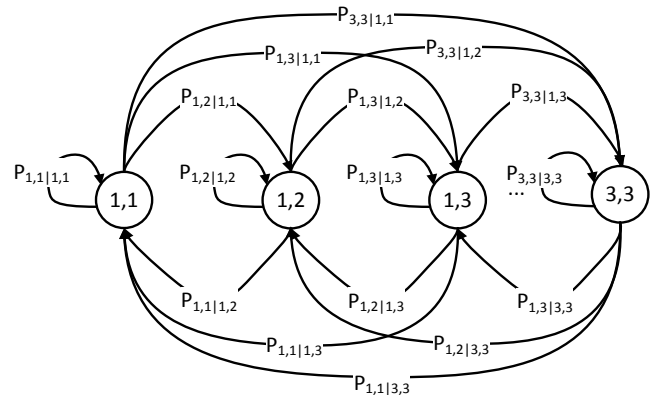


Figure 4: Multi-order generalization of the Markov chain model for the toy example.

For a set of cascade encoding sequences, let \mathbb{T} denote the set of selected orders as per the aforementioned criterion. We select the maximum value in \mathbb{T} , denoted by T_{max} , as the order of a single Markov chain model that we want to employ.

3.5 Cascade Classification

As mentioned in Section 1.2, an important desirable property for our proposed model is to identify differentiating features of cascade morphology that can be potentially leveraged for automated classification of cascades. We now show how to use the aforementioned Markov chain model to classify cascades.

3.5.1 Feature Selection

The essence of our modeling approach is to capture the morphology of a cascade through the states of the multi-order Markov model. Each state in the Markov chain represents a likely sub-structure of cascades' morphology. Thus, we can use these states to serve as underlying features that can be used to characterize a given cascade and to determine the class that it might belong to. However, as mentioned earlier, the number of states in a Markov chain increase exponentially for higher orders and so does the complexity of the underlying model. Furthermore, higher order Markov

chains require a large amount of training data to identify a subset of states that actually appear in the training data. In other words, a Markov chain model trained with limited data is typically sparse. Therefore, we use the following two approaches to systematically reduce the number of states in the Markov chain of order T_{max} .

First, we can combine multiple states in the Markov chain to reduce its number of states. By combining states in a multi-order Markov chain, we are essentially using states from lower order Markov chains. We need to establish a criterion to combine states in the Markov chain. Towards this end, we use the concept of *typicality* of Markov chain states. Typicality allows us to identify a typical subset of Markov chain states by generating its realizations [5]. Before delving into further details, we first state the well-known typicality theorem below: For any stationary and irreducible Markov process X and a constant c , the sequence x_1, x_2, \dots, x_m is almost surely (n, ϵ) -typical for every $n \leq c \log m$ as $m \rightarrow \infty$. A sequence x_1, x_2, \dots, x_m is called (n, ϵ) -typical for a Markov process X if $\hat{P}(x_1, x_2, \dots, x_n) = 0$, whenever $P(x_1, x_2, \dots, x_n) = 0$, and

$$\left| \frac{\hat{P}(x_1, x_2, \dots, x_n)}{P(x_1, x_2, \dots, x_n)} - 1 \right| < \epsilon, \text{ when } P(x_1, x_2, \dots, x_n) > 0.$$

Here $\hat{P}(x_1, x_2, \dots, x_n)$ and $P(x_1, x_2, \dots, x_n)$ are the empirical relative frequency and the actual probability of the sequence x_1, x_2, \dots, x_n , respectively. In other words,

$$\hat{P}(x_1, x_2, \dots, x_n) \approx P(x_1, x_2, \dots, x_n).$$

This theorem shows us a way of empirically identifying typical sample paths of arbitrary length for a given Markov process. Based on this theorem, we generate realizations (or sample paths) of arbitrary lengths from the transition matrix of the Markov process. By generating a sufficiently large number of sample paths of a given length, we can identify a relatively small subset of sample paths that are typical. Using this criterion, we select a subset of up to top-100,000 typical states as potential features, whose lengths vary in the range $[0, T_{max}]$. In what follows, we further short-list the Markov states from the top-100,000 typical subset and use them as features to classify cascades.

Second, to further reduce the number of features to be employed in a classifier, we need to prioritize the aforementioned typical Markov states. The prioritization of features can be based on their differentiation power. An information theoretic measure that can be used to quantify the differentiation power of features (Markov states in our case) is information gain [7]. In this context, information gain is the mutual information between a given feature X_i and the class variable Y . For a given feature X_i and the class variable Y , the information gain of X_i with respect to Y is defined as:

$$IG(X_i; Y) = H(Y) - H(Y|X_i),$$

where $H(Y)$ denotes the marginal entropy of the class variable Y and $H(Y|X_i)$ represents the conditional entropy of Y given feature X_i . In other words, information gain quantifies the reduction in the uncertainty of the class variable Y given that we have complete knowledge of the feature X_i . Note that, in this paper, the class variable Y is $\{0, 1\}$ because we apply our morphology modeling framework to problems that require differentiating between two classes of cascades (as described later). In this study, we eventually only select the top-100 features with highest information gain.

3.5.2 Classification

Let us assume that the presence of a state i is represented by a binary random variable $X_i, i = 1, 2, \dots, 100$. Hence, $P(X_i = 1)$ represents the probability for the presence of state X_i . We can think of the X_i s as the variables representing potential features. Thus, our training process proceeds as follows. For a given class Y of cascades, we evaluate the presence of a given feature (state) X_i in Y by analyzing a sufficiently large number of sample cascades that belong to the class Y . Subsequently, we are able to evaluate the a-priori conditional probability $P(X_i|Y)$ for each class $Y \in \{1, 2, \dots, k\}$, where the number of classes k is usually very small. In our case, we are interested in the traditional binary classifier with $k = 2$. However, note that this classification methodology can be extended to the cases with $k > 2$ using the well-known one-against-one (pairwise) or multiple one-against-all formulations [17].

We can jointly use multiple features to differentiate between two sets of cascades belonging to different classes. In particular, given the top-100 features with respect to information gain, we can classify cascades by deploying a machine learning classifier. In this study, we use a Bayesian classifier to jointly utilize the selected features to classify cascades. Naïve Bayes is a popular probabilistic classifier that has been widely used in the text mining and bio-informatics literature, and is known to outperform more complex techniques in terms of classification accuracy [35]. It trains using two sets of probabilities: the prior, which represents the marginal probability $P(Y)$ of the class variable Y ; and the a-priori conditional probabilities $P(X_i|Y)$ of the features X_i given the class variable Y . As previously explained, these probabilities can be computed from the training set.

Now, for a given test instance of a cascade with observed features $X_i, i = 1, 2, \dots, n$, the *a-posteriori* probability $P(Y|X^{(n)})$ can be computed for both classes $Y \in \{0, 1\}$, where $X^{(n)} = (X_1, X_2, \dots, X_n)$ is the vector of observed features in the test cascade under consideration:

$$P(Y|X^{(n)}) = \frac{P(X^{(n)}, Y)}{P(X^{(n)})} = \frac{P(X^{(n)}|Y)P(Y)}{P(X^{(n)})} \quad (3)$$

The naïve Bayes classifier then combines the a-posteriori probabilities by assuming conditional independence (hence the “naïve” term) among the features.

$$P(X^{(n)}|Y) = \prod_{i=1}^n P(X_i|Y). \quad (4)$$

Although the independence assumption among features makes it feasible to evaluate the a-posteriori probabilities with much lower complexity, it is unlikely that this assumption truly holds all the time. For our study, we mitigate the effect of the independence assumption by pre-processing the features using the well-known Karhunen-Loeve Transform (KLT) to uncorrelate them [9].

In the following section, we provide details of the data set that we have collected to demonstrate the usefulness of our M^4C model.

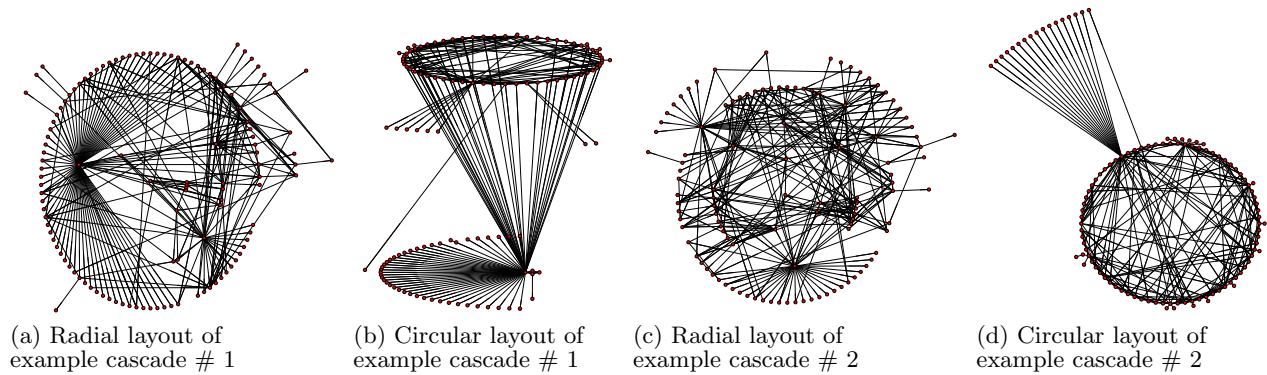


Figure 5: Typical examples of real-world Twitter cascades.

4. DATA SET

4.1 Data Collection

Among the popular online social networks, Twitter is one of the social networks that allows systematic collection of public data from its site. Therefore, we chose to study the morphology of cascades appearing on Twitter. To collect data from Twitter, we focused on tweets related to the Arab Spring event, which represents an ideal case study because it spans several months. For countries involved in the Arab Spring event, we collected data from Twitter during one complete week in March 2011. We provide more details of the data collection process in the following text.

For our study, we separately collected two data sets from Twitter. The first data set was collected using Twitter’s *streaming API*, which allows the realtime collection of public tweets matching one or more filter predicates [2]. To collect tweet data pertaining to a given country, we provided relevant keywords as filter predicates. For example, we used the keywords ‘Libya’ and ‘Tripoli’ to collect tweets related to Libya. In total, we collected tweets for 8 countries over a period of a week in March 2011. Using Twitter’s streaming API, we collected more than 8 million tweets involving more than 200 thousand unique users.

As mentioned in Section 3.1, we cannot accurately construct cascade graphs without information about whom the users are following. The one-way following policy of Twitter results in three types of relationships between two given users: (1) both follow each other, (2) only one of them follows the other, and (3) they do not follow each other. Twitter provides follower information for a given user via a separate interface called REST API [2]. REST API employs aggressive rate limiting by allowing clients to make only a limited number of API calls in an hour. Twitter applies this limit based on the public IP address or authentication token from the client who issues the request. Currently, rate limiting for REST API permits only 150 requests per hour for unauthenticated users and 350 requests per hour for authenticated users. In our tweet data set, we encountered more than 200,000 unique users and we were required to make at least one request per user to get the follower list. For each user who follows more than 5000 users, we had to make a separate call to get each subset of 5000 users. Here it is noteworthy that some users were following or were being followed by millions of users, requiring thousands of separate

calls for each user. It would take us several months to collect this data if we were to use a single authentication token or a single external IP address. To overcome this limitation, we utilized dozens of public proxy servers to parallelize calls to Twitter’s REST API [34]. Using this methodology, we collected follower lists of all users in less than a month.

Twitter provides a “re-tweet” functionality which allows users to re-post the tweet of other users to their profiles. The reference to the user with original tweet is maintained in all subsequent re-tweets. There is no information on intermediate users in re-tweets. Using the follower graph, we constructed cascade graphs for all sets of re-tweets which are essentially cascades. Therefore, the overall graph is a union of all cascades in our data. In Figure 5, we visualize two cascades in our data set using radial and circular layout methods in Graphviz [1]. In a radial layout, we choose the user with original tweet as a center vertex (or root vertex in general) and the remaining vertices are put in concentric circles based on their proximity to the center vertex. In a circular layout, all components are plotted separately with their respective vertices in a circular format. Visualization of two example cascades provides us interesting insights about their morphology. From the first example, we observe that the degree of vertices typically decreases as their distance from the root vertex increases. However, for the second example, we observe that subsequent vertices have degrees comparable to the root vertex. In this paper, our aim is to capture such differences in an automated fashion using our proposed model.

4.2 Data Analysis

We now analyze the structural features of the cascades in our collected data set in terms of degree, path, and connectivity. Later in Section 5, we will use these features for baseline comparison with our proposed model in terms of classification accuracy. For structural features that can only be computed from undirected graphs, such as clustering coefficient and diameter, we compute them on the undirected versions of cascade graphs.

4.2.1 Degree Properties

We first jointly study the number of edges and the number of nodes for all cascades in our data set. The cascade graphs in our data set are connected and each user in the cascade graph has at least one inward or outward edge. Therefore, the number of edges in a cascade graph $|E|$ has the lower

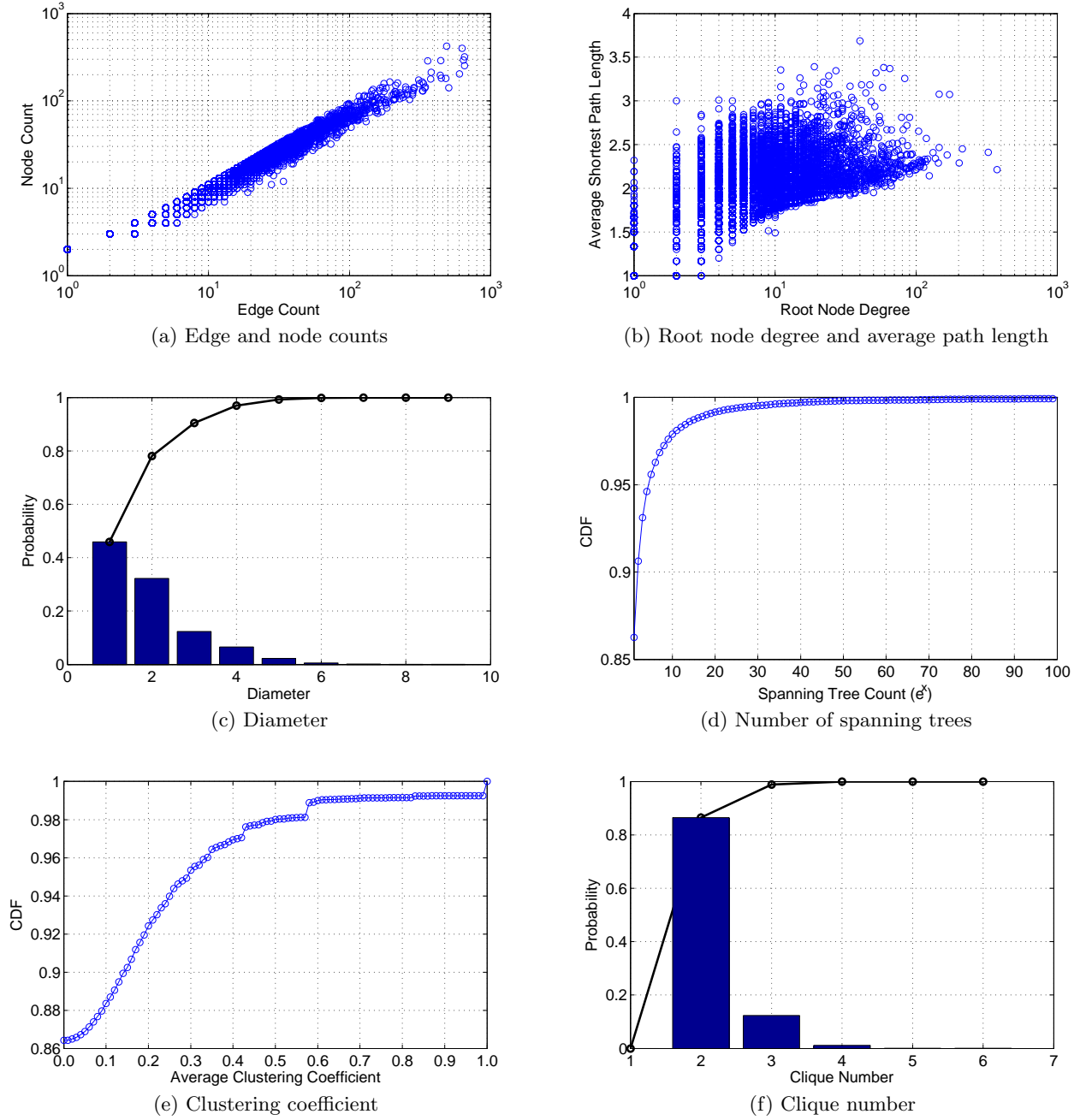


Figure 6: Distributions of various cascade graph attributes in the Twitter data set.

bound: $|E| \geq |V| - 1$, where $|V|$ is the number of users participating in the cascade. Figure 6(a) shows the scatter plot between edge and node counts for all cascades in our data set. Note that we use the logarithmic scale for both axes. From this figure, we observe that the scatter plot takes the form of a strip whose thickness represents the average number of additional edges for each node. The average thickness of this strip approximately corresponds to having twice the number of edges compared to the number of nodes.

4.2.2 Path Properties

Another important characteristic of a cascade is the degree of the root node (user who initiated the cascade), which typically has the highest degree compared to all other nodes in a cascade graph. In our data set, the root node has the highest degree compared to all other nodes in cascade graphs for more than 92% of the cascades. The degree of the root node essentially represents the number of different routes through which cascade propagates in an online social network. Note that these paths may merge together after the first hop; however, we expect some correlation between the degree of

root node and the number of unique routes through which a cascade propagates. One relevant characteristic of a graph is average (shortest) path length (APL), which denotes the average of all-pair shortest paths [4].

$$APL = \sum_{\forall i, j \in V, i \neq j} \frac{d(i, j)}{|V|(|V| - 1)},$$

where $d(i, j)$ is the shortest path length between users i and j . We expect the average path length of a cascade to be proportional to the degree of the root node. Figure 6(b) shows the scatter plot of the root node degree and the average path length. As expected, we observe that cascades with higher root node degrees tend to have larger average path lengths. We have changed the x-axis to logarithm scale to emphasize this relationship.

Another fundamental characteristic of a graph is called diameter, which denotes the largest value of all-pair shortest paths [4]. Figure 6(c) shows the distribution of diameter of cascades in our data set. The bars represent the probability mass function and the line represents the cumulative density function (CDF). The minimum diameter is 1 because the minimum number of nodes in a cascade is 2. Cascades with more than 2 nodes can have a diameter of 1 only if they are cliques. In our data set, approximately 40% cascades have a diameter of 1. The largest cascades in our data set have a diameter of 9.

Finally, we can characterize the number of unique paths that connect nodes in a graph by using the notion of spanning trees. For a given graph, the number of unique paths between nodes is proportional to the number of spanning trees. The number of spanning trees of a graph G , denoted by $t(G)$, is given by the product of non-zero eigenvalues of the Laplacian matrix and the reciprocal of the number of nodes [4].

$$t(G) = \frac{1}{n} \lambda_1 \lambda_2 \dots \lambda_{n-1},$$

where n is the number of nodes of the graph and λ_i is the i -th eigenvalue of the Laplacian matrix of the graph and $\lambda_i \neq 0, \forall i$. Figure 6(d) shows the CDF of the number of spanning trees for cascades in our data set. Note that the x-axis is converted to logarithm scale. We observe that only a small fraction ($< 15\%$) of cascades have more than one spanning tree in our data set, which highlights their sparsity.

4.2.3 Connectivity Properties

The clustering coefficient of a vertex v_i is denoted by c_i and is defined as the ratio of the number of existing edges among v_i and v_i 's neighbors and the number of all possible edges among them [4]. Using Δ_i to denote the number of triangles containing vertex v_i and d_i to denote the degree of vertex v_i , the clustering coefficient of vertex v_i is defined as:

$$c_i = \frac{\Delta_i}{\binom{d_i}{2}} = \frac{2\Delta_i}{d_i(d_i - 1)}$$

The average clustering coefficient of a graph G with n nodes is simply the mean of clustering coefficients of individual nodes.

$$C_{avg} = \frac{1}{n} \sum_{\forall i} c_i$$

Figure 6(e) shows the CDF of the average clustering coefficient for all cascades in our data set. We note that approximately 86% of all cascades in our data set have average

clustering coefficient value equal to 0, *i.e.*, they do not have a single triangle. Only a small fraction (less than 2%) of cascades in our data set have clustering coefficient values greater than 0.5, which again highlights their sparsity.

We are also interested in investigating the sizes of cliques in cascades that have one or more triangles. Towards this end, we study the clique numbers of all cascade graphs in our data set. The clique number of a graph is the number of vertices in its largest clique [4]. Figure 6(f) shows the distribution of clique number for all cascades in our data set. Similar to our observation in Figure 6(e), we observe that approximately 86% of cascades have a clique number of 2, which means that they do not have a triangle. A little more than 10% of cascades have at least one triangle. The largest clique number observed in our data set is 6.

5. CASCADE SIZE PREDICTION

To demonstrate the effectiveness of our M^4C model in quantitatively characterizing cascades, we use it to investigate an unexplored but fundamental problem in online social networks - *cascade size prediction: given the first τ_1 edges in a cascade, we want to predict whether the cascade will have a total of at least τ_2 ($\tau_2 > \tau_1$) edges over its lifetime*. Besides serving the purpose of validating the relevance of our M^4C model, this prediction has many real-world applications. For instance, it is useful for media organizations to forecast popular news stories [15]. Likewise, popular videos on social media – if predicted early – can be cached by content distribution networks at their servers to achieve better performance [29]. Furthermore, solving this problem enables the early detection of epidemic outbreaks and political crisis.

To the best of our knowledge, this problem has not been investigated in prior literature. The closest effort is that Galuba *et al.* analyzed the cascades of URLs on Twitter to predict URLs that users will tweet [12]. Their proposed approach achieved about 50% true positive rate with about 15% false positive rate. Unfortunately, this accuracy is not much useful in practice.

We compare the prediction performance of M^4C based scheme with a baseline scheme that uses the following 8 cascade graph features with Naïve Bayes classifier: (1) edge growth rate, (2) number of nodes, (3) degree of the root node, (4) average shortest path length, (5) diameter, (6) number of spanning trees, (7) clustering coefficient, and (8) clique number. We evaluate the effectiveness of these schemes in terms of the following decision sets.

1. *True Positives (TPs)*: The set of cascades that are correctly predicted to have a total of at least τ_2 edges over their lifetime.
2. *False Positives (FPs)*: The set of cascades that are incorrectly predicted to have a total of at least τ_2 edges over their lifetime.
3. *True Negatives (TNs)*: The set of cascades that are correctly predicted to have a total of less than τ_2 edges over their lifetime.
4. *False Negatives (FNs)*: The set of cascades that are incorrectly predicted to have a total of less than τ_2 edges over their lifetime.

We further quantify the effectiveness of both cascade size prediction schemes in terms of the following three Receiver

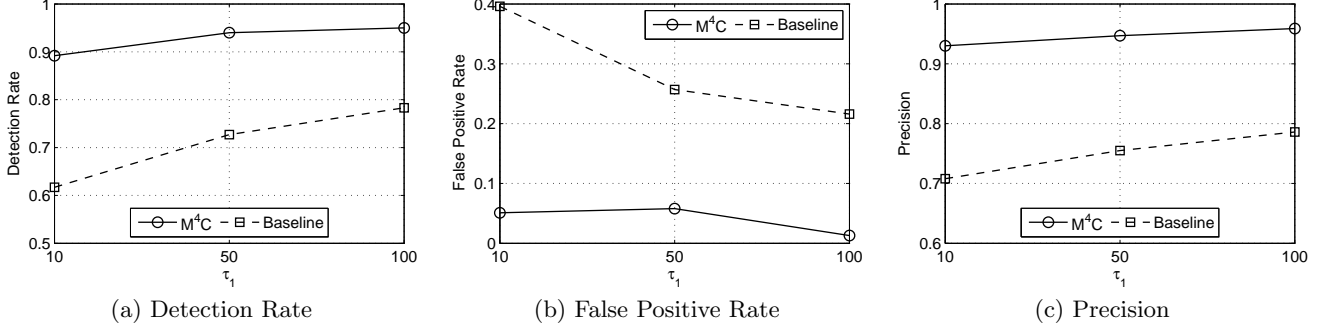


Figure 7: Classification results of M^4C and baseline schemes for varying values of τ_1 , at $\tau_2 - \tau_1 = 10$.

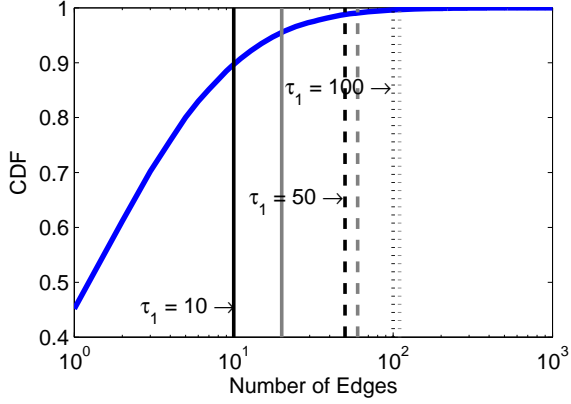


Figure 8: Evaluation setup for varying τ_1 .

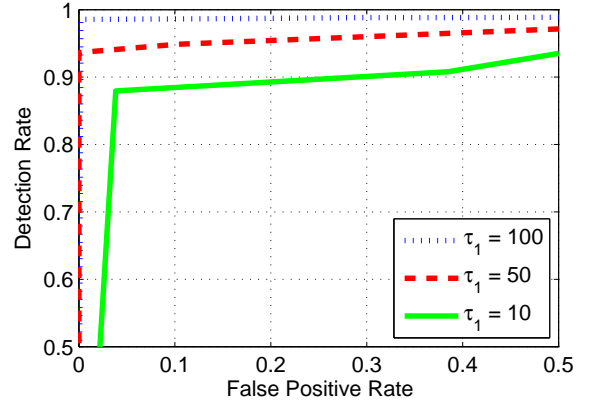


Figure 9: ROC plot of M^4C based scheme for varying τ_1 .

Operating Characteristic (ROC) metrics [11].

$$\text{Detection Rate} = \frac{|TPs|}{|TPs| + |FNs|} \quad (5)$$

$$\text{False Positive Rate} = \frac{|FPs|}{|FPs| + |TNs|} \quad (6)$$

$$\text{Precision} = \frac{|TPs| + |TNs|}{|TPs| + |TNs| + |FPs| + |FNs|} \quad (7)$$

To ensure that the classification results are generalizable, we divide the data set into k folds and use $k - 1$ of them for training and the left over for testing. We repeat these experiments k times and report the average results in the following text. This setup is called stratified k -fold cross-validation procedure [35]. For all experimental results reported in this paper, we use the value of $k = 10$.

In this paper, we treat the cascade size prediction problem to an equivalent cascade classification problem: given a cascade with τ_1 edges, classify it into two classes: the class of cascades that will have less than τ_2 edges over their lifetime and the class of cascades that will have greater than or equal to τ_2 edges over their lifetime. We use the initial τ_1 edges to train both the cascade size prediction scheme based on our M^4C model and the baseline scheme that is based on the known cascade graph features. For thorough evaluation, we vary the values of τ_1 and τ_2 . Because the distribution of the number of edges in our data set is skewed, that is, most cascades having only a few edges over their lifetime, the larger

the values of τ_1 and $\tau_2 - \tau_1$ are, the more imbalanced the two classes are. To mitigate the potential adverse effect of class imbalance [18], we employ instance re-sampling to ensure that both classes have equal number of instances before the cross-validation evaluations. Below we discuss the classification accuracies of both schemes as we vary the values of τ_1 and τ_2 .

5.1 Impact of Varying τ_1

Figure 8 shows the evaluation setup as we vary the values of $\tau_1 \in \{10, 50, 100\}$, while keeping $\tau_2 - \tau_1$ fixed at 10. The solid, dashed, and dotted vertical black lines corresponds to $\tau_1 = 10, 50$, and 100. The solid, dashed, and dotted vertical grey lines all correspond to $\tau_2 - \tau_1 = 10$. The value of τ_1 impacts the classification results because it determines the number of edges in each cascade that are available for training. Therefore, larger values of τ_1 generally improve training quality of both cascade size prediction schemes and lead to better prediction accuracy.

Figure 7 plots the detection rate, false positive rate, and precision of M^4C and baseline schemes for varying $\tau_1 \in \{10, 50, 100\}$, while keeping $\tau_2 - \tau_1$ fixed at 10. Overall, we observe that M^4C consistently outperforms the baseline scheme with peak precision of 96% at $\tau_1 = 100, \tau_2 - \tau_1 = 10$ s. With some exceptions, we generally observe that the effectiveness of both schemes decreases as the value of τ_1 is in-

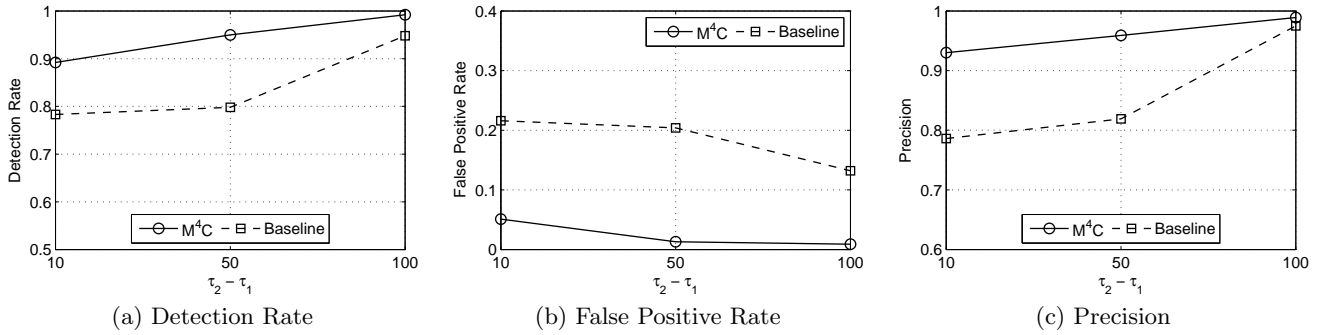


Figure 11: Classification results of M^4C and baseline schemes for varying values of $\tau_2 - \tau_1$, at $\tau_1 = 10$.

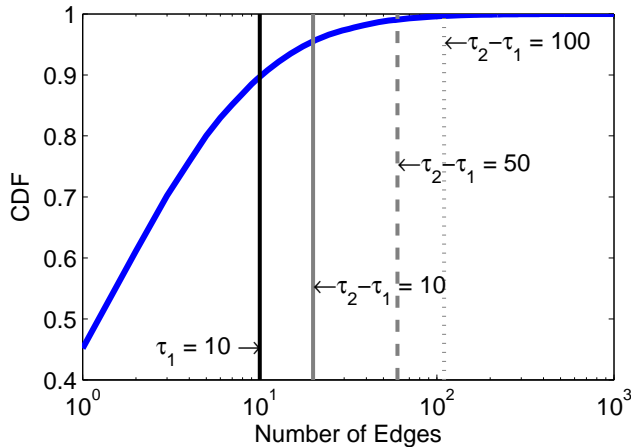


Figure 10: Evaluation setup for varying $\tau_2 - \tau_1$.

created. The standard ROC threshold plots of M^4C shown in Figure 9 also confirm this observation.

5.2 Impact of Varying $\tau_2 - \tau_1$

Figure 10 shows the evaluation setup as we vary the values of $\tau_2 - \tau_1 \in \{10, 50, 100\}$, while keeping τ_1 fixed at 10. The solid vertical black line corresponds to $\tau_1 = 10$. The solid, dashed, and dotted vertical grey lines correspond to $\tau_2 - \tau_1 = 10, 50$, and 100, respectively. The value of $\tau_2 - \tau_1$ also impacts the classification results because it determines the separation or distance between the two classes. Therefore, larger values of $\tau_2 - \tau_1$ generally lead to better prediction accuracy.

Figure 11 plots the detection rate, false positive rate, and precision of M^4C and baseline schemes for varying values of $\tau_2 - \tau_1$. Once again, we observe that M^4C consistently outperforms the baseline scheme with peak precision of 99% at $\tau_2 - \tau_1 = 100, \tau_1 = 10$. We also observe that the classification performance of both methods improves as the value of $\tau_2 - \tau_1$ is increased. The standard ROC threshold plots of M^4C shown in Figure 12 also confirm this observation.

6. CONCLUSIONS AND FUTURE WORK

In this paper, we first propose M^4C , a multi-order Markov chain based model to represent and quantitatively charac-

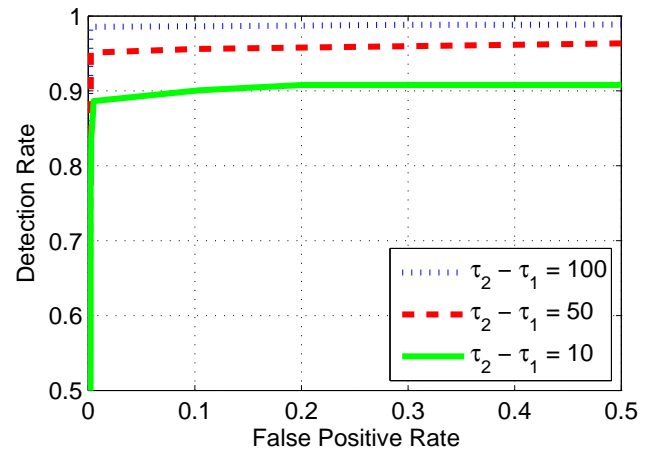


Figure 12: ROC plot of M^4C based scheme for varying $\tau_2 - \tau_1$.

terize the morphology of cascades with arbitrary structures, shapes, and sizes. We then demonstrate the relevance of our M^4C model in solving the cascade size prediction problem. The experimental results using a real-world Twitter data set showed that M^4C significantly outperforms the baseline scheme in terms of prediction accuracy. In summary, our M^4C model allows us to formally and rigorously study cascade morphology, which is otherwise difficult.

In this paper, we applied our M^4C model in the context of online social networks; however, our model is generally applicable to cascades in other contexts as well such as sociology, economy, psychology, political science, marketing, and epidemiology. Applications of our model in these contexts are interesting future work to pursue.

7. REFERENCES

- [1] Graphviz - graph visualization software. <http://www.graphviz.org>.
- [2] Twitter API documentation. <https://dev.twitter.com/docs>.
- [3] A. Biem. Minimum classification error training for online handwriting recognition. *IEEE Transactions on Pattern Analysis and Machine Intelligence*, 28:1041–1051, 2006.

- [4] A. Bondy and U. Murty. *Graph Theory*. Springer, 2008.
- [5] P. Bremaud. *Markov Chains*. Springer, 2008.
- [6] M. Cha, A. Mislove, and K. P. Gummadi. A measurement-driven analysis of information propagation in the Flickr social network. In *ACM WWW*, 2009.
- [7] T. M. Cover and J. A. Thomas. *Elements of Information Theory*. Wiley-Interscience, 1991.
- [8] K. Dave, R. Bhatt, and V. Varma. Modelling action cascades in social networks. In *AAAI Conference on Weblogs and Social Media*, 2011.
- [9] R. Dony. *The Transform and Data Compression Handbook, Chapter 1*. CRC Press, 2001.
- [10] T. Douglas. Social media’s role in the riots. BBC news, August 2011.
- [11] T. Fawcett. ROC Graphs: Notes and Practical Considerations for Researchers. Technical report, HP Laboratories, 2004.
- [12] W. Galuba, K. Aberer, D. Chakraborty, Z. Despotovic, and W. Kellerer. Outtweeting the twitterers - predicting information cascades in microblogs. In *Workshop on Online Social Networks*, 2010.
- [13] V. Gomez, H. J. Kappen, and A. Kaltenbrunner. Modeling the structure and evolution of discussion cascades. In *ACM HT*, 2011.
- [14] M. Gomez-Rodriguez, J. Leskovec, and A. Krause. Inferring networks of diffusion and influence. In *ACM KDD*, 2010.
- [15] D. Gruhl, R. Guha, R. Kumar, J. Novak, and A. Tomkins. The predictive power of online chatter. In *ACM KDD*, 2005.
- [16] S.-Y. Hsieha, C.-W. Huang, and H.-H. Choub. A DNA-based graph encoding scheme with its applications to graph isomorphism problems. *Applied Mathematics and Computation*, 203:502–512, 2008.
- [17] C.-W. Hsu and C.-J. Lin. A comparison of methods for multiclass support vector machines. *IEEE Transactions on Neural Networks*, 13(2):415–425, 2002.
- [18] N. Japkowicz and S. Stephen. The class imbalance problem: A systematic study. *Intelligent Data Analysis*, 6(5):429–449, 2002.
- [19] N. S. Jayant and P. Noll. *Digital Coding of Waveforms: Principles and Applications to Speech and Video*. Prentice Hall, 1984.
- [20] D. Kempe, J. Kleinberg, and E. Tardos. Maximizing the spread of influence through a social network. In *proceedings of KDD*, 2003.
- [21] S. A. Khayam and H. Radha. Markov-based modeling of wireless local area networks. In *ACM Mobicom Workshop on Modeling, Analysis and Simulation of Wireless and Mobile Systems*, 2003.
- [22] H. Kwak, C. Lee, H. Park, and S. Moon. What is Twitter, a social network or a news media? In *ACM WWW*, 2010.
- [23] J. Leskovec, M. McGlohon, C. Faloutsos, N. Glance, and M. Hurst. Cascading behavior in large blog graphs. In *SIAM International Conference on Data Mining (SDM)*, 2007.
- [24] J. Leskovec, A. Singh, and J. Kleinberg. Patterns of influence in a recommendation network. In *Pacific-Asia Conference on Knowledge Discovery and Data Mining (PAKDD)*, 2006.
- [25] X. Li. Informational cascades in IT adoption. *Communications of the ACM*, 47(4), 2004.
- [26] M. Miller, C. Sathi, D. Wiesenhal, J. Leskovec, and C. Potts. Sentiment flow through hyperlink networks. In *AAAI ICWSM*, 2011.
- [27] T. Ray. The ‘story’ of digital excess in revolutions of the arab spring. *Journal of Media Practice*, 12(2):189–196, 2011.
- [28] M. Reid, R. Millar, and N. D. Black. Second-generation image coding: An overview. *Second-Generation Image Coding: An Overview*, 29:3–29, 1997.
- [29] T. Rodrigues, F. Benevenuto, M. Cha, K. P. Gummadi, and V. Almeida. On word-of-mouth based discovery of the web. In *ACM IMC*, 2011.
- [30] E. M. Rogers. *Diffusion of Innovations*. Cambridge University Press, 2003.
- [31] D. M. Romero, B. Meeder, and J. Kleinberg. Differences in the mechanics of information diffusion across topics: Idioms, political hashtags, and complex contagion on Twitter. In *ACM WWW*, 2011.
- [32] E. Sadikov, M. Medina, J. Leskovec, and H. Garcia-Molina. Correcting for missing data in information cascades. In *WSDM*, 2011.
- [33] J. A. Starr and I. C. MacMillan. Resource cooptation via social contracting: Resource acquisition strategies for new ventures. *Strategic Management Journal*, 11:79–92, 1990.
- [34] L. Wang, K. Park, R. Pang, V. Pai, and L. Peterson. Reliability and security in the CoDeeN content distribution network. In *USENIX Annual Technical Conference*, 2004.
- [35] I. H. Witten, E. Frank, and M. A. Hall. *Data Mining: Practical Machine Learning Tools and Techniques*. Morgan Kaufmann, 2011.
- [36] Z. Zhou, R. Bandar, J. Kong, H. Qian, and V. Roychowdhury. Information resonance on Twitter: Watching Iran. In *SOMA*, 2010.